
Influence of ferric iron dosing on aerobic granular sludge: granule formation, nutrient removal and microbial community

Jinte Zou^{a,b}, Fengfan Yu^b, Jia Chen^b, Giorgio MANNINA^{a,c}, Yongmei Li^{a,d*}

^a State Key Laboratory of Pollution Control and Resource Reuse, College of Environmental Science and Engineering, Tongji University, Shanghai, 200092, China

^b Key Laboratory of Microbial Technology for Industrial Pollution Control of Zhejiang Province, College of Environment, Zhejiang University of Technology, Hangzhou 310014, China

^c Engineering Department, Palermo University, Viale delle Scienze, Ed. 8, 90128, Palermo, Italy

^d Shanghai Institute of Pollution Control and Ecological Security, Shanghai 200092, P.R. China

* Corresponding author: Tel: +86 21 65982692; Fax: +86 21 65986313; E-mail: liyongmei@tongji.edu.cn

Abstract

BACKGROUND: Three lab-scale sequencing batch reactors were used to investigate the effects of Fe³⁺ on aerobic granular sludge (AGS) formation, nutrient removal, and microbial community.

RESULTS: The addition of 6 and 12 mg Fe³⁺/L could not shorten the granulation time. However, compared to the reactor without Fe³⁺ addition (average sludge volume index at 30 min (SVI₃₀): 70.8 mL/g; stable average particle size: 548 μm), the addition of 12 mg Fe³⁺/L helped improve the physical properties of AGS (average SVI₃₀: 57.0

This article has been accepted for publication and undergone full peer review but has not been through the copyediting, typesetting, pagination and proofreading process which may lead to differences between this version and the [Version of Record](#). Please cite this article as doi: [10.1002/jctb.6640](https://doi.org/10.1002/jctb.6640)

mL/g; stable average particle size: 1067 μm). Furthermore, with 12 mg Fe^{3+} /L addition (Fe^{3+} to $\text{PO}_4^{3-}\text{-P}$ molar ratio=1.33), good removals of $\text{NH}_4^+\text{-N}$ (≤ 0.5 mg/L) and $\text{PO}_4^{3-}\text{-P}$ (< 1 mg/L) were achieved. The addition of Fe^{3+} reduced the microbial diversity and specific activity of heterotrophic bacteria, but promoted the growth of nitrite-oxidizing bacteria. The growth of particle size not only increased the active biomass ratio and microbial diversity, but alleviated the inhibition effect of Fe^{3+} on the specific heterotrophic bacteria activity.

CONCLUSION: The addition of Fe^{3+} had both negative and positive effects on the formation and stability of AGS. The results will help enrich the understanding of AGS application in nutrient especially phosphorus removal.

Keywords: Aerobic granular sludge; ferric iron; phosphorus and nitrogen removal; microbial community; microbial activity

INTRODUCTION

Aerobic granular sludge (AGS) is a promising technology that has attracted lots of attention from researchers due to its excellent settling property, high biomass retention, small footprint, and potential to remove nitrogen and phosphorus (P) simultaneously (Wu et al., 2012; Nancharaiah and Reddy, 2018; Zou et al., 2018).¹⁻³ Extensive works have been conducted to better understand the mechanisms of AGS formation and stability.³⁻⁶ The crystalline nuclei and selection pressure are widely regarded as the two main factors affecting sludge granulation.^{2,7} Extracellular polymeric substances (EPS) are also considered to play an important role in AGS formation and stability.^{8,9} In addition, with more and more stringent requirement for

Accepted Article

nutrient discharge from wastewater treatment plants (WWTPs), P removal are usually achieved by combining chemical and biological methods. Ferric salt is one of the most common chemical flocculants used in WWTPs to remove P.¹⁰ Recently, some full-scale applications of AGS around the world have been reported.^{11,12} Therefore, it is meaningful to study the effects of ferric ion (Fe^{3+}) on AGS formation, nutrient removal, and microbial community.

Generally, Fe^{3+} added to the mixed liquor will react with phosphate and hydroxide ions to form insoluble ferric phosphate precipitates and hydroxide complexes which will subsequently assist in P removal by adsorption and co-precipitation.¹³ The ferric phosphate precipitates and ferric hydroxide complexes are reported to have poor settleability, which will result in an unfavourable settling velocity for the activated sludge.^{14,15} The decline of sludge settleability due to the addition of Fe^{3+} may adversely affect the sludge granulation process. However, on the other hand, metal ions can stimulate sludge granulation by neutralizing the negative cell surface charge, polymer bridging of EPS, forming precipitates onto which cells can aggregate.^{8,16,17} Therefore, the actual effect of Fe^{3+} on AGS formation needs to be studied deeply. Recently, Kończak et al.¹⁶ studied the synergetic effect of Ca^{2+} (5 mg/L), Mg^{2+} (3 mg/L) and Fe^{3+} (4.2 mg/L) addition on the formation and structure of AGS, but the effect of Fe^{3+} was not deeply investigated. Their study also indicated that Fe^{3+} promoted the secretion of protein (PN) and could bind with EPS similarly to divalent cations.¹⁶ By adding Fe^{2+} (1 and 10 mg/L) to the feed solution and reactor, Yilmaz et al.¹⁸ noted that iron ions ($\text{Fe}^{2+}/\text{Fe}^{3+}$) increased the size and stability of AGS, but did

not affect the granulation time. In activated sludge systems, Liu et al.¹⁹ found that the effects of Fe³⁺ and Fe²⁺ on biological P removal and nitrification were weak, and these iron salts inhibited P removal only when the dose was large enough (> 40mg/L). However, Liu and Horn²⁰ reported that nitrogen removal was evidently deteriorated during the deammonification process when Fe³⁺ concentrations were increased from 0.75 to 2.19 mg/L. To the best of our knowledge, studies related the impacts of Fe³⁺ on AGS formation and performance are still very limited.

This study aims to investigate the effects of Fe³⁺ on AGS formation, nutrient removal, and microbial community. Two levels of Fe³⁺ (6 and 12 mg/L) were tested in the sequencing batch reactors (SBRs). Biomass concentration, sludge settleability, particle size, EPS content, chemical precipitates content, reactor performance, microbial activity, and community were monitored during the experimental period. The results of this study will help enrich the understanding of AGS application in nutrient especially P removal.

MATERIALS AND METHODS

Reactor setup and operation

Three identical plexiglas SBRs (R1, R2, and R3) with the internal diameter of 10 cm and the effective height to diameter ratio of 8.9 were used. The effective working volume of each reactor was 7 L. Bottom aeration was supplied with an airflow rate of 7.0 L/min, and the volumetric exchange ratio was 50%. The temperature in the reactors was around 16 ± 2 °C during the experimental period. The reactors were all operated with a 4-h cycle, consisting of feeding (4 min), aeration (180 min), settling

(4-30 min), decanting (2 min), and idling (24-50 min). Thus, the hydraulic retention time was 8 h. In order to investigate the effect of Fe^{3+} on AGS formation and performance, a concentrated FeCl_3 solution was added to R2 and R3 to obtain the initial concentrations of 6 and 12 mg Fe^{3+}/L , respectively. To completely mix the FeCl_3 solution and sludge, the FeCl_3 solution was added after 5 min of aeration. The adding time for each cycle was 1 min, and the adding volume was controlled by a peristaltic pump. R1 without extra Fe^{3+} addition served as the control. The Fe^{3+} concentrations selected in this study were based on a preliminary batch test for chemical removal of P (data not shown).

Synthetic wastewater with the following composition was used: 512 mg of sodium acetate (400 mg/L as chemical oxygen demand (COD) basis), 21.9 mg of KH_2PO_4 and 36.8 mg of $\text{K}_2\text{HPO}_4 \cdot 3\text{H}_2\text{O}$ (10 mg/L as $\text{PO}_4^{3-}\text{-P}$ basis), 172.0 mg of NH_4Cl (45 mg/L as $\text{NH}_4^+\text{-N}$ basis), 88.6 mg of $\text{MgSO}_4 \cdot 7\text{H}_2\text{O}$ (8.6 mg/L as Mg basis), 111.0 mg of CaCl_2 (40 mg/L as Ca basis), and 0.3 mL of trace solution per liter. The trace solution consisted of the following compounds per liter: 1.5 g of $\text{FeCl}_3 \cdot 6\text{H}_2\text{O}$, 0.15 g of H_3BO_3 , 0.03 g of $\text{CuSO}_4 \cdot 5\text{H}_2\text{O}$, 0.18 g of KI, 0.12 g of $\text{MnCl}_2 \cdot 4\text{H}_2\text{O}$, 0.06 g of $\text{Na}_2\text{MoO}_4 \cdot 2\text{H}_2\text{O}$, 0.12 g of $\text{ZnSO}_4 \cdot 7\text{H}_2\text{O}$, 0.15 g of $\text{CoCl}_2 \cdot 6\text{H}_2\text{O}$, and 10 g of EDTA.²¹

The seed sludge was taken from a municipal WWTP in Shanghai, in which an anaerobic-anoxic-aerobic process was used for nutrient removal. The sludge volume index at 5 min (SVI_5) and sludge volume index at 30 min (SVI_{30}) for the seed sludge were 210.5, and 191.2 mL/g, respectively. The initial concentration of mixed liquor suspended solid (MLSS) in each reactor was approximately 4655 mg/L. Fe^{3+} was

added in each cycle after one day of cultivation. In order to avoid the excessive biomass wash-out, the settling time decreased stepwise from 30 min to 5 min based on the sludge settleability in each reactor (Fig. 1). During the experimental period, the biomass wastage was not controlled in all the reactors but occurred through sludge washout during the decanting phase.

Additionally, a batch experiment was conducted to evaluate the particle size of the iron precipitates and hydrolyzates. Specifically, a 1-L beaker filled with 0.1 M Tris-HCl buffer (pH 8.1) was used. A concentrated phosphate solution was added to achieve the initial $\text{PO}_4^{3-}\text{-P}$ concentration of 5 mg/L. Then, a concentrated FeCl_3 solution was added to each beaker to achieve the initial Fe^{3+} concentrations of 6 or 12 mg/L. Finally, the particle size was measured after one hour of reaction.

Analytical methods

COD, $\text{NH}_4^+\text{-N}$, $\text{NO}_2^-\text{-N}$, $\text{NO}_3^-\text{-N}$, $\text{PO}_4^{3-}\text{-P}$, total nitrogen (TN), total phosphate, MLSS, mixed liquor volatile suspended solid (MLVSS), pH, SVI_5 , and SVI_{30} were measured according to the Standard Methods.²² The size of sludge was monitored by laser diffraction (Mastersizer 3000, Malvern, UK) with tap water as the suspension medium and standard optical parameters (main statistical size parameters: D10, D50 and D90 indicate that 10 %, 50 % and 90 % of the total particle volume have a smaller particle size than the D10, D50 and D90, respectively).²³ X-ray diffraction (XRD) analysis was performed using a D8 Advance diffractometer (Bruker, Germany) with a ceramic tube scattering from 10° to 90° in 2θ . In order to remove the organic fraction, samples were dried and calcined in an oven at 500°C for 2 h before XRD

analysis. The AGS morphology was observed via digital camera and scanning electron microscopy (SEM) according to the method described by Li et al.²⁴ Energy dispersive X-ray (EDX) combined with SEM was used to analyze the element composition of precipitates adhered to AGS. The contents of P, Ca, Mg and Fe in sludge were analyzed using an inductively coupled plasma emission spectrometer (ICP 720ES, Agilent, USA) after sludge digestion according to the method reported by Ščančar et al.²⁵ The EPS of sludge samples was extracted using a heat method.²³ The polysaccharide (PS) content in EPS was quantified using the anthrone method.²⁶ The PN content in EPS was also quantified using a reagent kit (Sangon Biotech, China) based on the bicinchoninic acid method.²⁷

Measurement of microbial activity and microbial community

Batch experiments were performed to evaluate the specific oxygen uptake rate (SOUR) of bacteria (including ammonia-oxidizing bacteria (AOB), nitrite-oxidizing bacteria (NOB), and heterotrophic bacteria (HB)), and the maximum specific oxidation rates of $\text{NH}_4^+\text{-N}$ and $\text{NO}_2^-\text{-N}$ in each reactor. The measurements of SOUR_{AOB} , SOUR_{NOB} , and SOUR_{HB} were according to the method described by Liu et al.¹⁹ The measurements of maximum specific oxidation rates of $\text{NH}_4^+\text{-N}$ and $\text{NO}_2^-\text{-N}$ can be found elsewhere.²³

Seed sludge and sludge of R1, R2, and R3 on day 80 were used to analyze the characterization of microbial community. DNA was extracted from sludge using the E.Z.N.A.[®] Tissue DNA Kit (Omega Bio-tek, UAS) according to manufacturer's protocols. The DNA was checked on 1% agarose gel, and DNA quality was

determined through OD_{260/280}. The primers for bacteria were 338F (5'-ACTCCTACGGGAGGCAGCAG-3') and 806R (5'-GGACTACHVGGGTWTCTAAT-3'). The detailed polymerase chain reaction amplification, Illumina Miseq sequencing and processing of sequencing data were conducted according to the reported protocol.²⁸ The raw sequencing data of bacteria have been deposited in the GenBank database under the accession number SRR3538700.

Statistical analysis

An analysis of variation (ANOVA) was used to evaluate the significance of results, and $p < 0.05$ was considered to be statistically significant.

RESULTS AND DISCUSSION

Formation and characterization of AGS

As shown in Fig. 1(a), MLSS and MLVSS sharply decreased on day 1 in all the three reactors due to the reduction of settling time from 30 min to 7-12 min. After that, MLSS and MLVSS in R1 gradually increased, and SVI gradually decreased. On day 20, the SVI₅ and SVI₃₀ in R1 decreased to 74.7 and 69.3 mL/g, respectively, and the ratio of SVI₃₀/SVI₅ and D50 were 0.93 and 370 μm , respectively (Fig. 1). According to the previous study, granulation is deemed to be completed when the ratio of SVI₃₀/SVI₅ is higher than 0.9 and at the same time, a clear outline of sludge is observed.²⁹ Thus, it is assumed that the granulation time in R1 was 20 days. In R2, the SVI₅ and SVI₃₀ were higher than 100 mL/g in the first 32 days, and D50 was lower than 200 μm in the first 55 days. Furthermore, the ratio of SVI₃₀/SVI₅ was always

Accepted Article

lower than 0.9 during the whole experiment (Fig. S1). These results indicated that the addition of 6 mg Fe³⁺/L was adverse to the sludge granulation. In R3, MLSS and MLVSS increased rapidly after 32 days of cultivation. On day 35, the SVI₅ and SVI₃₀ decreased to 63.1 and 60.8 mL/g, respectively, and the ratio of SVI₃₀/SVI₅ and D50 increased to 0.96 and 721 μm, respectively. Therefore, it is assumed that the granulation time in R3 was 35 days. The settling time was longer in R3 (12 min) than in R1 (6-7 min) in the first 43 days (Fig. 1(a)). This is probably the main reason for the longer granulation time in R3 because the longer settling time resulted in a longer granulation time.³⁰ However, the average SVI₅ and SVI₃₀ in R3 after granulation were 60.9 and 57.0 mL/g, respectively, which were lower than those in R1 (SVI₅: 75.4 mL/g; SVI₃₀: 70.8 mL/g). The average particle size in the steady period in R3 was 1067 μm, which was larger than that in R1 (548 μm). These results indicate that although the addition of 12 mg Fe³⁺/L could not shorten the granulation time, it helped improve the settleability and particle size of AGS.

It should be noted that D10 in R2 was always very low (< 60 μm) (Fig. 1(b)). Similar phenomenon was also observed in R3 in the first 32 days (< 50 μm). The low value of D10 in R2 and R3 should be attributed to the Fe³⁺ addition, leading to the formation of iron precipitates and hydrolyzates with small particle size. The particle size determination by a batch experiment without biomass confirmed that the iron precipitates and hydrolyzates had a very small particle size (D50 < 15 μm) (Table S1). The iron precipitates and hydrolyzates also have poor settleability, possibly because PO₄³⁻-P is loosely bound to the Fe(OH)₃ flocs.¹⁴ Consequently, the addition of Fe³⁺ in

R2 and R3 adversely affected the sludge settleability due to the formation of iron precipitates and hydrolyzates with poor settleability. Similar phenomenon was also observed in other researches.¹⁵ The results that the effluent SS and VSS in R2 and R3 were still higher than those in R1 even when the settling time was longer in R2 and R3 at the beginning of cultivation (Fig. S2) further supported this conclusion. The poor sludge settleability at the beginning would adversely affect the granulation process. On the other hand, the PS content was almost at the same level in R1 (10.4 ± 1.3 mg/gVSS), R2 (9.1 ± 1.6 mg/gVSS) and R3 (11.8 ± 3.4 mg/gVSS) during the experimental period (Fig. 2). However, the PN content in R2 and R3 was always higher than that in R1 during the whole experiment. The maximum PN contents in R2 and R3 were 132.2 and 109.2 mg/gVSS, respectively, while it was only 70.8 mg/gVSS in R1. Generally, microbial cells in sludge produced more EPS in the presence of toxic substances.³¹ The addition of 6 and 12 mg Fe³⁺/L might have some toxicity to the sludge as indicated by the inhibition of microbial activity (Table 1, discussed in section of Microbial community and activity). Therefore, the addition of Fe³⁺ increased the PN production in EPS. The PN in EPS positively affects the cell hydrophobicity and settleability, and high PN content in EPS benefits the formation and stability of AGS.^{8,9} Therefore, the addition of Fe³⁺ has a positive effect on AGS formation and stability by improving the PN content in sludge EPS.

Variation of chemical precipitates

The ratio of MLVSS/MLSS in R1 increased from 0.83 (day 1) to 0.93 (day 16), and then stabilized within this range (Fig. S1). The increase in MLVSS/MLSS ratio might

Accepted Article

be attributed to the fact that the inorganic salts concentration in the synthetic wastewater was less than that in the real municipal wastewater.⁴ However, the ratio of MLVSS/MLSS in R2 rapidly decreased to 0.76 (day 5), and then stabilized at around 0.79. The rapid decrease in MLVSS/MLSS ratio was attributed to the addition of Fe^{3+} , leading to the accumulation of iron precipitates and hydrolyzates on sludge. Additionally, the ratio of MLVSS/MLSS in R3 was lower than that in R2 in the first 32 days. This was mainly due to the higher dose of Fe^{3+} in R3. However, about 35 days later, the ratio of MLVSS/MLSS was higher in R3 than in R2. The increase in the ratio of active biomass in R3 might be attributed to the increase in particle size of AGS.

As shown in Fig. 3 (a), the contents of Ca, Mg, Fe, and P in sludge in R2 were always higher than those in R1 during the whole experiment. Similar phenomenon was also observed in R3 in the first 46 days. These results indicate that the addition of Fe^{3+} increased the contents of inorganic precipitates in sludge. The SEM-EDX analysis also supported this conclusion. Some tiny particles containing metal elements of Ca and Fe were observed in AGS of R2 and R3, but not in AGS of R1 (Fig. S3). XRD analysis showed that the detected minerals in sludge samples of R2 and R3 were hematite (Fe_2O_3) and calcium pyrophosphate ($\text{Ca}_2\text{P}_2\text{O}_7$) (Fig. S4). Moreover, srebrodolskite ($\text{Ca}_2\text{Fe}_2\text{O}_5$) was found in sludge sample of R2, while iron phosphate hydroxide ($\text{Fe}_3(\text{PO}_4)_2(\text{OH})_3$) in sludge sample of R3. Since $\text{Fe}(\text{OH})_3$ can be transformed to Fe_2O_3 at 500 °C,³² the main hydrolyzate in the original sludge samples of R2 and R3 should be $\text{Fe}(\text{OH})_3$. In addition, the contents of Ca, Mg, Fe, and P in

Accepted Article

sludge in R3 were much higher than those in R2 at the beginning of cultivation due to the higher dose of Fe^{3+} in R3. The high contents of inorganic precipitates in sludge at the beginning of cultivation could improve the sludge specific density and serve as nuclei, and thereby alleviate the adverse effect of Fe^{3+} on sludge settleability. This might be the main reason that complete granulation was observed in R3 with 12 mg Fe^{3+} /L addition, but not in R2 with 6 mg Fe^{3+} /L addition. Moreover, the contents of Ca, Mg, Fe, and P in sludge in R3 exhibited a decreasing trend during the granulation process. After 32 days of cultivation, these elements in sludge in R3 were all lower than those in R2. Thus, it indicates that the increase in particle size in R3 helped to increase the active biomass ratio of AGS. The main reason is probably that AGS with large particle size has lower specific surface area, adsorption cumulative volume of pores, and adsorption average pore width in comparison to the AGS with small particle size,²⁶ leading to a lower adsorption of chemical precipitates onto the AGS with large particle size.

As shown in Fig. 3 (b), the contents of Ca and Mg in sludge of different size (5.4 ± 0.6 and 3.7 ± 0.1 mg/gVSS) were relatively stable in R1; whereas the contents of Fe and P in sludge gradually decreased as the particle size increased from 50-150 to 300-500 μm (statistical difference as $p < 0.05$). In R2, the contents of Ca, Fe, and P in sludge decreased significantly as the particle size increased from < 50 to 150-300 μm (statistical difference as $p < 0.05$). However, when the particle size was greater than 150-300 μm , they became relatively stable. Similarly, a significant decrease in the contents of Ca, Mg, Fe, and P in sludge was observed in R3 when the particle size

increased from < 50 to $300\text{-}500\ \mu\text{m}$ (statistical difference as $p < 0.05$). Nevertheless, they were relatively stable when the particle size was greater than $300\text{-}500\ \mu\text{m}$. These results further confirm that the particle size growth resulted in the decrease in precipitates and hydrolyzates contents of AGS.

Performance of the reactors

The concentrations of COD and $\text{NH}_4^+\text{-N}$ in the effluent in R1, R2, and R3 during the experiment were 42 ± 11 and 0.5 ± 0.5 , 37 ± 10 and 0.3 ± 0.3 , 37 ± 10 and 0.5 ± 0.9 mg/L, respectively (Fig. 4). Thus, good removals of COD and $\text{NH}_4^+\text{-N}$ were achieved in all the reactors during the experimental period. The concentrations of COD and $\text{NH}_4^+\text{-N}$ in the effluent during the experiment showed no statistical difference in R1, R2, and R3 ($p > 0.05$), which indicates that the addition of Fe^{3+} had no significant effect on the removal performance of COD and $\text{NH}_4^+\text{-N}$. Additionally, the pH value in the effluent fluctuated within the range of 7.7-8.6 during the whole experiment in R1, R2, and R3 (Fig. S5). The highest pH values in R1, R2, and R3 in one typical cycle were 9.2, 8.8, and 9.0, respectively, and the highest concentrations of free ammonia (FA) were 7.2, 3.2, and 5.2 mg/L, respectively (Fig. S5). It is generally accepted that both AOB and NOB are inhibited by FA, but the NOB is more sensitive to FA than AOB, giving the inhibition range of 0.1-1.0 mg/L and 10-150 mg/L, respectively.³³ Thus, nitrite accumulation was observed in all the reactors. The occurrence of partial nitrification in AGS system resulting from the high pH value and FA concentration was also reported by Li et al..²⁴ However, nitrite accumulation completely disappeared in R2 and R3 in 60 days. This indicates that the addition of

Accepted Article

Fe^{3+} was detrimental to the partial nitrification in AGS system. During the experimental period, the effluent pH value in R1 was in the range of 8.1-8.6, which was higher than that in R2 (7.8-8.3) and R3 (7.7-8.3) (Fig. S5). Meanwhile, the maximum concentration of FA in one typical cycle in R1 was 7.2 mg/L, which was higher than that in R2 (3.2 mg/L) and R3 (5.2 mg/L) (Fig. S5). Therefore, the inhibition of FA on NOB activity was weaker in R2 and R3 than in R1. Thus, partial nitrification gradually disappeared in R2 and R3. At the steady period (day 62 to day 83), the average removals of TN in R1, R2, and R3 were 42.5%, 30.3%, and 51.1%, respectively. These values were lower than the results in our previous studies,^{6,24} which was probably due to the lower COD concentration in the influent. Moreover, the removed nitrogen amount via simultaneous nitrification-denitrification in the aeration phase in R1, R2, and R3 were 11.4, 0.0, and 32.3 mg, respectively, which accounted for 19.5%, 0.0%, and 32.3% of the total removed nitrogen in a typical cycle (Table S2). Therefore, the higher TN removal in R3 may be attributed to the larger particle size, leading to more anoxic zones for denitrification during the aeration phase.^{24,34}

As shown in Fig. 4(b), the concentration of $\text{PO}_4^{3-}\text{-P}$ in the effluent significantly decreased with the addition of Fe^{3+} (statistical difference as $p < 0.05$). The concentrations of $\text{PO}_4^{3-}\text{-P}$ in the effluent in R1, R2, and R3 during the experiment were 8.6 ± 0.7 , 3.5 ± 0.4 and 0.9 ± 0.1 mg/L, respectively, and the average removal efficiencies were 17.8%, 66.5% and 91.0%, respectively. Considering the volumetric exchange ratio (50%) in this study, the actual molar ratios of Fe^{3+} to $\text{PO}_4^{3-}\text{-P}$ in R2 and

R3 were 0.66 and 1.33, respectively. Therefore, good removal of $\text{PO}_4^{3-}\text{-P}$ ($< 1 \text{ mg/L}$) was achieved in AGS system when the molar ratio of Fe^{3+} to $\text{PO}_4^{3-}\text{-P}$ was greater than 1.33. This is consistent with the study in activated sludge systems.³⁵

Microbial community and activity

The high-throughput sequencing was used to investigate the microbial community in seed sludge, sludge of R1, R2, and R3. The coverage in all the sludge samples was greater than 99%, indicating that microbial community could be well represented by the collected gene sequences. The indexes of Ace, Chao and Shannon in seed sludge (274, 274, and 4.48) were higher than those in R1 (222, 233, and 3.31), R2 (200, 213, and 1.79), and R3 (217, 216, and 2.85), and the index of Simpson in seed sludge (0.0294) was lower than that in R1 (0.0828), R2 (0.4790), and R3 (0.1176). This indicates that the microbial richness and diversity decreased after the formation of AGS. This result is in agreement with the previous study.³⁶ Moreover, the indexes of Ace, Chao, and Shannon in all the sludge samples were ranked as follows: $\text{R1} > \text{R3} > \text{R2}$. The index of Simpson was ranked as $\text{R1} < \text{R3} < \text{R2}$. Consequently, the addition of Fe^{3+} reduced the microbial richness and diversity, but the growth of particle size increased the microbial richness and diversity.

At the phylum level, *Proteobacteria* was the most abundant phylum in seed sludge, sludge of R1, R2, and R3, accounting for 41.7%, 77.7%, 85.3%, and 66.3%, respectively (Fig. 5(a)). *Bacteroidetes* was the second dominant phylum in the four sludge samples (39.1%, 19.7%, 12.8%, and 31.0%, respectively). This is consistent with our previous study stating that *Proteobacteria* and *Bacteroidetes* are the

commonly predominant phyla in AGS system.⁶ At the genus level, the most abundant genus in seed sludge was *Saprospiraceae_uncultured* (23.6%), followed by *Comamonadaceae_unclassified* (15.3%) and *Dokdonella* (6.0%) (Fig. 5(b)). However, they all showed a declining trend in sludge of R1, R2, and R3. The differences of microbial community between the seed sludge and sludge of R1 were probably due to the formation of AGS and the use of synthetic wastewater and aerobic SBR in this study.³⁷ In addition, the main genera in R1 were *DBI-14_norank* (20.8%), *Azoarcus* (15.9%), *Zoogloea* (15.3%), and *Cytophagaceae_uncultured* (7.0%). However, they became *Zoogloea* (68.8%) and *Saprospiraceae_uncultured* (6.0%) in R2, and *Zoogloea* (20.2%), *Thauera* (20.1%), *Saprospiraceae_uncultured* (13.5%), *Alcaligenaceae_uncultured* (10.6%), *Flavobacterium* (7.5%), and *Cytophagaceae_uncultured* (5.3%) in R3. Therefore, the addition of Fe³⁺ influenced the structure of microbial community, which was also reported by Ren et al.³⁸ As shown in Fig. 5(c), the relative abundances of AOB in R2 (0.3%) and R3 (0.4%) were lower than that in R1 (0.9%). Nevertheless, the relative abundances of NOB in R2 (1.1%) and R3 (4.3%) were higher than that in R1 (0.2%). Thus, the addition of Fe³⁺ gradually inhibited the growth of AOB, but stimulated the growth of NOB (mainly *Candidatus_Nitrotoga*³⁹). Similar phenomenon was also observed in other study with the addition of 10 mg Fe²⁺/L.⁴⁰ The inhibition of Fe³⁺ on AOB growth was one of the reasons that partial nitrification gradually disappeared in R2 and R3.

As shown in Table 1, the SOUR_{AOB} and maximum specific oxidation rate of NH₄⁺-N in R3 (8.5 ± 0.6 mgO₂/(gVSS·h) and 2.0 ± 0.3 mgN/(gVSS·h)) were lower

than those in R1 ($10.4 \pm 0.8 \text{ mgO}_2/(\text{gVSS}\cdot\text{h})$ and $2.5 \pm 0.2 \text{ mgN}/(\text{gVSS}\cdot\text{h})$) (statistical difference as $p < 0.05$). However, they showed no statistical difference in R2 and R1 ($p > 0.05$). This result indicates that the significant decrease in the specific activity of AOB occurred when the long-term addition of Fe^{3+} was 12 mg/L. The SOUR_{NOB} and maximum specific oxidation rate of NO_2^- -N in R2 ($9.9 \pm 0.3 \text{ mgO}_2/(\text{gVSS}\cdot\text{h})$ and $1.9 \pm 0.2 \text{ mgN}/(\text{gVSS}\cdot\text{h})$) and R3 ($10.0 \pm 0.2 \text{ mgO}_2/(\text{gVSS}\cdot\text{h})$ and $2.1 \pm 0.2 \text{ mgN}/(\text{gVSS}\cdot\text{h})$) were higher than those in R1 ($2.3 \pm 0.4 \text{ mgO}_2/(\text{gVSS}\cdot\text{h})$ and $0.5 \pm 0.1 \text{ mgN}/(\text{gVSS}\cdot\text{h})$) (statistical difference as $p < 0.05$). This was probably related to the relatively weaker inhibition of FA on NOB activity when 6 or 12 mg Fe^{3+}/L was added, resulting in the growth of NOB in R2 and R3 in the long run (Fig. 5(c)). Additionally, the SOUR_{HB} in R3 ($34.7 \pm 1.0 \text{ mgO}_2/(\text{gVSS}\cdot\text{h})$) was lower than that in R1 ($52.5 \pm 0.9 \text{ mgO}_2/(\text{gVSS}\cdot\text{h})$), but higher than that in R2 ($24.2 \pm 0.4 \text{ mgO}_2/(\text{gVSS}\cdot\text{h})$) (statistical difference as $p < 0.05$). This indicates that the long-term addition of Fe^{3+} might reduce the specific activity of HB, but the growth of particle size could help alleviate the inhibition. Generally, AOB mainly reside in the outer layer of AGS, while some heterotrophic denitrifying bacteria usually reside in the inner layer of AGS.⁴¹ Therefore, the inhibition effect of Fe^{3+} on the specific activity of HB could be alleviated due to the substrate limitation resulting from the large particle size of AGS. Although the specific activity of AOB and HB in R2 and R3 decreased due to the long-term addition of Fe^{3+} , the removal performance of COD and NH_4^+ -N was not affected during the experimental period.

CONCLUSION

The addition of Fe^{3+} had both negative and positive effects on the formation and stability of AGS. On the one hand, the addition of Fe^{3+} adversely affected sludge granulation due to the formation of iron precipitates and hydrolyzates with poor settleability. On the other hand, the addition of Fe^{3+} increased the contents of precipitates as crystalline nuclei in sludge at the beginning of cultivation, and the PN content in EPS, which were beneficial to the formation and stability of AGS. Granulation time was not shortened with the addition of 6 and 12 mg Fe^{3+}/L , but the addition of 12 mg Fe^{3+}/L helped improve the settleability and particle size of AGS (average SVI_{30} : 57.0 mL/g; stable average particle size: 1067 μm) compared to the reactor without Fe^{3+} addition (average SVI_{30} : 70.8 mL/g; stable average particle size: 548 μm). Additionally, good removals of $\text{NH}_4^+\text{-N}$ (≤ 0.5 mg/L) and $\text{PO}_4^{3-}\text{-P}$ (< 1 mg/L) were achieved after granulation with the addition of 12 mg Fe^{3+}/L (Fe^{3+} to $\text{PO}_4^{3-}\text{-P}$ molar ratio=1.33). The addition of Fe^{3+} reduced the microbial diversity and specific activity of HB, but promoted the growth of NOB. The particle size growth not only increased the active biomass ratio and microbial diversity, but alleviated the inhibition effect of Fe^{3+} on the specific HB activity.

ACKNOWLEDGEMENTS

This work was supported by the National Natural Science Foundation of China (Grant no. 51708500), Zhejiang Xinmiao Talents Program (2019R403012), Shanghai Science and Technology Committee (No. 18230712100) and the Fundamental Research Funds for the Central Universities (22120190202).

REFERENCES

1 Wu CY, Peng YZ, Wang SY, Ma Y, Enhanced biological phosphorus removal by granular sludge: From macro- to micro-scale. *Water Res* **44**: 807-814 (2010).

2 Zou JT, Tao YQ, Li J, Wu SY, Ni YJ, Cultivating aerobic granular sludge in a developed continuous-flow reactor with two-zone sedimentation tank treating real and low-strength wastewater. *Bioresour Technol* **247**: 776-783 (2018).

3 Nancharaiah YV, Reddy GKK, Aerobic granular sludge technology: Mechanisms of granulation and biotechnological applications. *Bioresour Technol* **247**: 1128-1143 (2018).

4 Su KZ, Yu HQ, Formation and characterization of aerobic granules in a sequencing batch reactor treating soybean-processing wastewater. *Environ Sci Technol* **39**: 2818-2827 (2005).

5 Gao D, Liu L, Liang H, Wu WM, Aerobic granular sludge: characterization mechanism of granulation and application to wastewater treatment. *Crit Rev Biotechnol* **31**: 137-152 (2011).

6 Zou JT, Pan JY, Wu SY, Qian MJ, He ZF, Wang BB, Li J, Rapid control of activated sludge bulking and simultaneous acceleration of aerobic granulation by adding intact aerobic granular sludge. *Sci Total Environ* **647**: 105-113 (2019).

7 Li J, Liu J, Wang DJ, Chen T, Ma T, Wang ZH, Zhuo WL, Accelerating aerobic sludge granulation by adding dry sewage sludge micropowder in sequencing batch reactors. *Int J Env Res Public Health* **12**: 10056-10065 (2015).

8 Liu Y, Liu Z, Wang F, Chen Y, Kuschk P, Wang X, Regulation of aerobic granular sludge reformulation after granular sludge broken: effect of poly aluminum chloride

(PAC). *Bioresour Technol* **158**: 201-208 (2014).

9 Zhu L, Zhou J, Lv M, Yu H, Zhao H, Xu X, Specific component comparison of extracellular polymeric substances (EPS) in flocs and granular sludge using EEM and SDS-PAGE. *Chemosphere* **121**: 26-32 (2015).

10 Wilfert P, Kumar PS, Korving L, Witkamp GJ, van Loosdrecht MCM, The relevance of phosphorus and iron chemistry to the recovery of phosphorus from wastewater: a review. *Environ Sci Technol* **49**: 9400-9414 (2015).

11 Li J, Ding LB, Cai A, Huang GX, Horn H, Aerobic sludge granulation in a fullscale sequencing batch reactor. *Biomed Res Int* 268789 (2014).

12 Pronk M, de Kreuk MK, de Bruin B, Kamminga P, Kleerebezem R, van Loosdrecht MCM, Full scale performance of the aerobic granular sludge process for sewage treatment. *Water Res* **84**: 207–217 (2015).

13 Mbamba CK, Lindblom E, Flores-Alsina X, Tait S, Anderson S, Saagi R, Batstone DJ, Gernaey KV, Jeppsson U, Plant-wide model-based analysis of iron dosage strategies for chemical phosphorus removal in wastewater treatment systems. *Water Res* **155**: 12-25 (2019).

14 Thistleton J, Berry TA, Pearce P, Parsons SA, Mechanisms of chemical phosphorus removal II - Iron(III) salts. *Process Saf Environ* **80**: 265-269 (2002).

15 Asensi E, Alemany E, Duque-Sarango P, Aguado D, Assessment and modelling of the effect of precipitated ferric chloride addition on the activated sludge settling properties. *Chem Eng Res Des* **150**: 14-25 (2019).

16 Kończak B, Karcz J, Miksch K, Influence of calcium, magnesium, and iron ions on

aerobic granulation. *Appl Biochem Biotechnol* **174**: 2910-2918 (2014).

17 Wilen BM, Liebana R, Persson F, Modin O, Hermansson M, The mechanisms of granulation of activated sludge in wastewater treatment, its optimization, and impact on effluent quality. *Appl Microbiol Biotechnol* **102**: 5005-5020 (2018).

18 Yilmaz G, Bozkurt U, Magden KA, Effect of iron ions (Fe^{2+} , Fe^{3+}) on the formation and structure of aerobic granular sludge. *Biodegradation* **28**: 53-68 (2017).

19 Liu Y, Shi H, Li W, Hou Y, He M, Inhibition of chemical dose in biological phosphorus and nitrogen removal in simultaneous chemical precipitation for phosphorus removal. *Bioresour Technol* **102**: 4008-4012 (2011).

20 Liu S, Horn H, Effects of Fe(II) and Fe(III) on the single-stage deammonification process treating high-strength reject water from sludge dewatering. *Bioresour Technol* **114**: 12-19 (2012).

21 Kishida N, Kim J, Tsuneda S, Sudo R, Anaerobic/oxic/anoxic granular sludge process as an effective nutrient removal process utilizing denitrifying polyphosphate-accumulating organisms. *Water Res* **40**: 2303-2310 (2006).

22 American Public Health Association (APHA), Standard methods for the examination of water and wastewater, twenty-second ed, APHA-AWWA-WEF, Washington, DC (2012).

23 Zou J, Li Y, Zhang L, Wang R, Sun J, Understanding the impact of influent nitrogen concentration on granule size and microbial community in a granule-based enhanced biological phosphorus removal system. *Bioresour Technol* **177**: 209-216 (2015).

- 24 Li YM, Zou JT, Zhang LL, Sun J, Aerobic granular sludge for simultaneous accumulation of mineral phosphorus and removal of nitrogen via nitrite in wastewater. *Bioresour Technol* **154**: 178-184 (2014).
- 25 Ščančar J, Milačič R, Horvat M, Comparison of various digestion and extraction procedures in analysis of heavy metals in sediments. *Water Air. Soil Pollut* **118**: 87-99 (2000).
- 26 Wu CY, Peng YZ, Wang RD, Zhou YX, Understanding the granulation process of activated sludge in a biological phosphorus removal sequencing batch reactor. *Chemosphere* **86**: 767-773 (2012).
- 27 Smith PK, Krohn RI, Hermanson GT, Mallia AK, Gartner FH, Provenzano MD, Fujimoto EK, Goeke NM, Olson BJ, Klenk DC, Measurement of protein using bicinchoninic acid. *Anal Biochem* **150**: 76-85 (1985).
- 28 Li YM, Wang J, Zhang A, Enhancing the quantity and quality of short-chain fatty acids production from waste activated sludge using CaO₂ as an additive. *Water Res* **83**: 84-93 (2015).
- 29 Liu YQ, Tay JH, Characteristics and stability of aerobic granules cultivated with different starvation time. *Appl Microbiol Biotechnol* **75**: 205-210 (2007).
- 30 Qin L, Liu Y, Tay JH, Effect of settling time on aerobic granulation in sequencing batch reactor. *Biochem Eng J* **21**: 47-52 (2004).
- 31 Sheng GP, Yu HQ, Li XY, Extracellular polymeric substances (EPS) of microbial aggregates in biological wastewater treatment systems: a review. *Biotechnol Adv* **28**: 882-894 (2010).

32 Sugimoto T, Sakata K, Muramatsu A, Formation mechanism of monodisperse pseudocubic α -Fe₂O₃ particles from condensed ferric hydroxide gel. *J Colloid Interf Sci* **159**: 372-382 (1993).

33 Zhang CS, Zhang SQ, Zhang LQ, Rong HW, Zhang KF, Effects of constant pH and unsteady pH at different free ammonia concentrations on shortcut nitrification for landfill leachate treatment. *Appl Microbiol Biot* **99**: 3707-3713 (2015).

34 Di Bella G, Torregrossa M, Simultaneous nitrogen and organic carbon removal in aerobic granular sludge reactors operated with high dissolved oxygen concentration. *Bioresour Technol* **142**: 706-713 (2013).

35 Caravelli AH, Contreras EM, Zaritzky NE, Phosphorous removal in batch systems using ferric chloride in the presence of activated sludges. *J Hazard Mater* **177**: 199-208 (2010).

36 Weissbrodt DG, Lochmatter S, Ebrahimi S, Rossi P, Maillard J, Holliger C, Bacterial selection during the formation of early-stage aerobic granules in wastewater treatment systems operated under wash-out dynamics. *Front Microbiol* **3**: 332 (2012).

37 He QL, Zhou J, Wang HY, Zhang J, Wei L, Microbial population dynamics during sludge granulation in an A/O/A sequencing batch reactor. *Bioresour Technol* **214**: 1-8 (2016).

38 Ren XM, Chen Y, Guo L, She ZL, Gao MC, Zhao YG, Shao MY, The influence of Fe²⁺, Fe³⁺ and magnet powder (Fe₃O₄) on aerobic granulation and their mechanisms. *Ecotox Environ Safe* **164**: 1-11 (2018).

39 Luecker S, Schwarz J, Gruber-Dorninger C, Spieck E, Wagner M, Daims H,

Nitrotoga-like bacteria are previously unrecognized key nitrite oxidizers in full-scale wastewater treatment plants. *Isme J* **9**: 708-720 (2015).

40 Yilmaz G, Cetin E, Bozkurt U, Magden KA, Effects of ferrous iron on the performance and microbial community in aerobic granular sludge in relation to nutrient removal. *Biotechnol Progr* **33**: 716-725 (2017).

41 Xia JT, Ye L, Ren HQ, Zhang XX, Microbial community structure and function in aerobic granular sludge. *Appl Microbiol Biotechnol* **102**: 3967-3979 (2018).

Table 1 Specific oxygen uptake rates (SOUR) and maximum specific oxidation rates of $\text{NH}_4^+\text{-N}$ and $\text{NO}_2^-\text{-N}$ in R1, R2, and R3 on day 76

Reactor	SOUR ($\text{mgO}_2/(\text{gVSS}\cdot\text{h})$)			Oxidation rates ($\text{mgN}/(\text{gVSS}\cdot\text{h})$)	
	AOB ^a	NOB ^b	HB ^c	$\text{NH}_4^+\text{-N}$	$\text{NO}_2^-\text{-N}$
R1	10.4 ± 0.8	2.3 ± 0.4	52.5 ± 0.9	2.5 ± 0.2	0.5 ± 0.1
R2	9.9 ± 0.3	9.9 ± 0.3	24.2 ± 0.4	2.3 ± 0.3	1.9 ± 0.2
R3	8.5 ± 0.6	10.0 ± 0.2	34.7 ± 1.0	2.0 ± 0.3	2.1 ± 0.2

^a ammonia-oxidizing bacteria, ^b nitrite-oxidizing bacteria, ^c heterotrophic bacteria

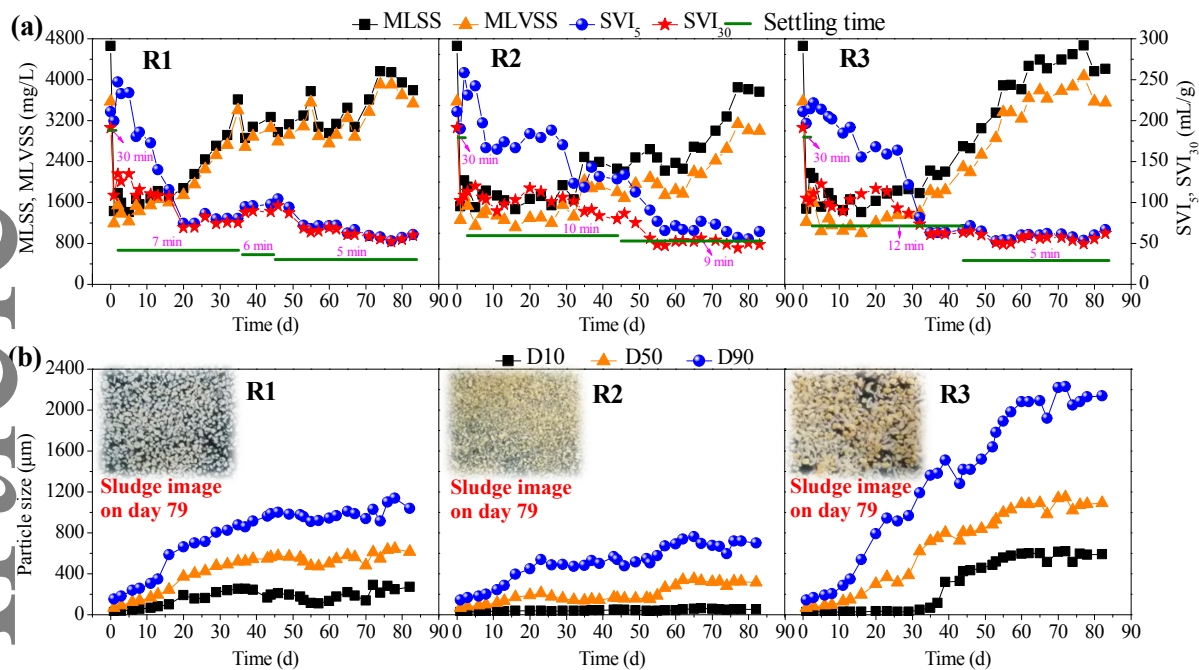


Fig. 1 Variations of MLSS, MLVSS, SVI₅, SVI₃₀, settling time (a), and particle size (b) in R1, R2, and R3 during the experimental period

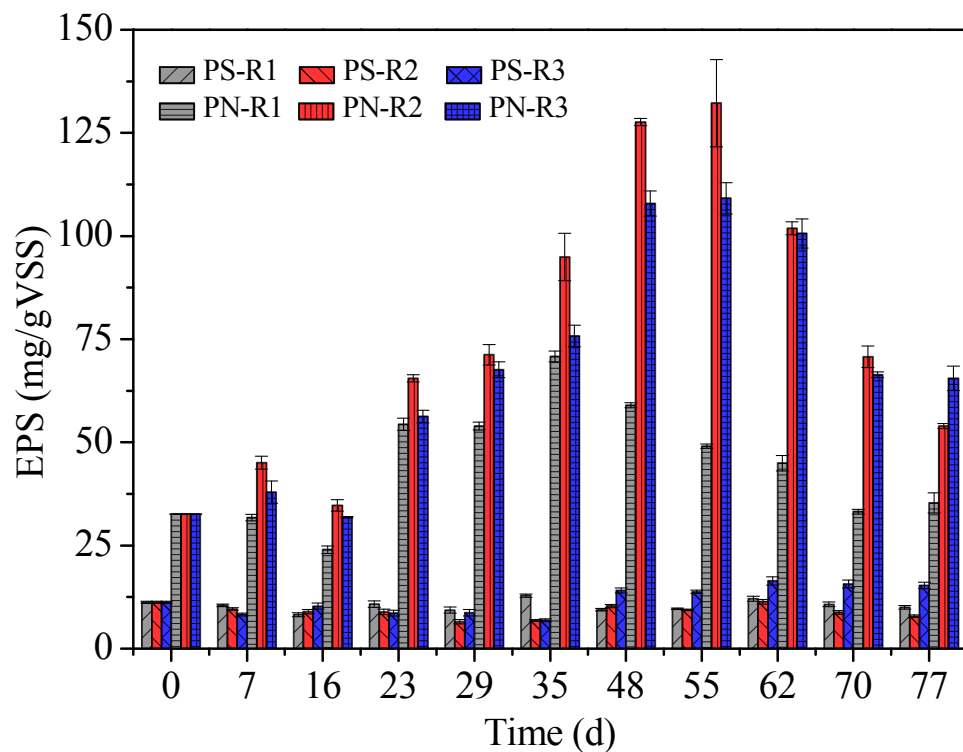


Fig. 2 Extracellular polymeric substances (EPS) variation in R1, R2, and R3 during the experimental period (PS: polysaccharides contents in EPS; PN: proteins content in EPS); error bars indicate the standard error of individual measurements (n=3)

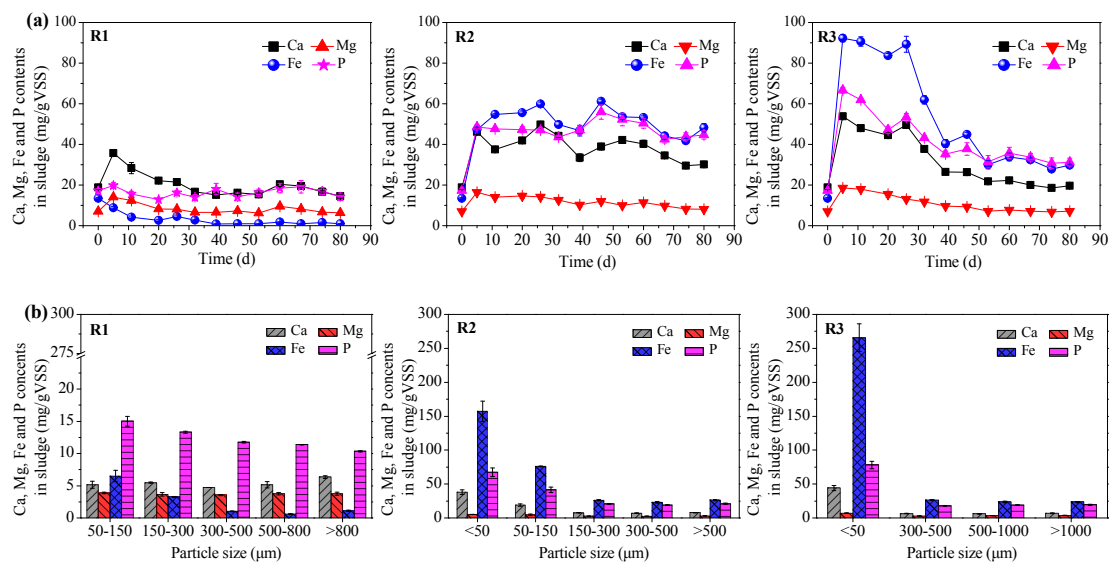


Fig.3 Variations of Ca, Mg, Fe and P contents in sludge in R1, R2, and R3 during the experimental period (a), and in sludge of different size in R1, R2, and R3 on day 81 (b); error bars indicate the standard error of individual measurements (n=3)

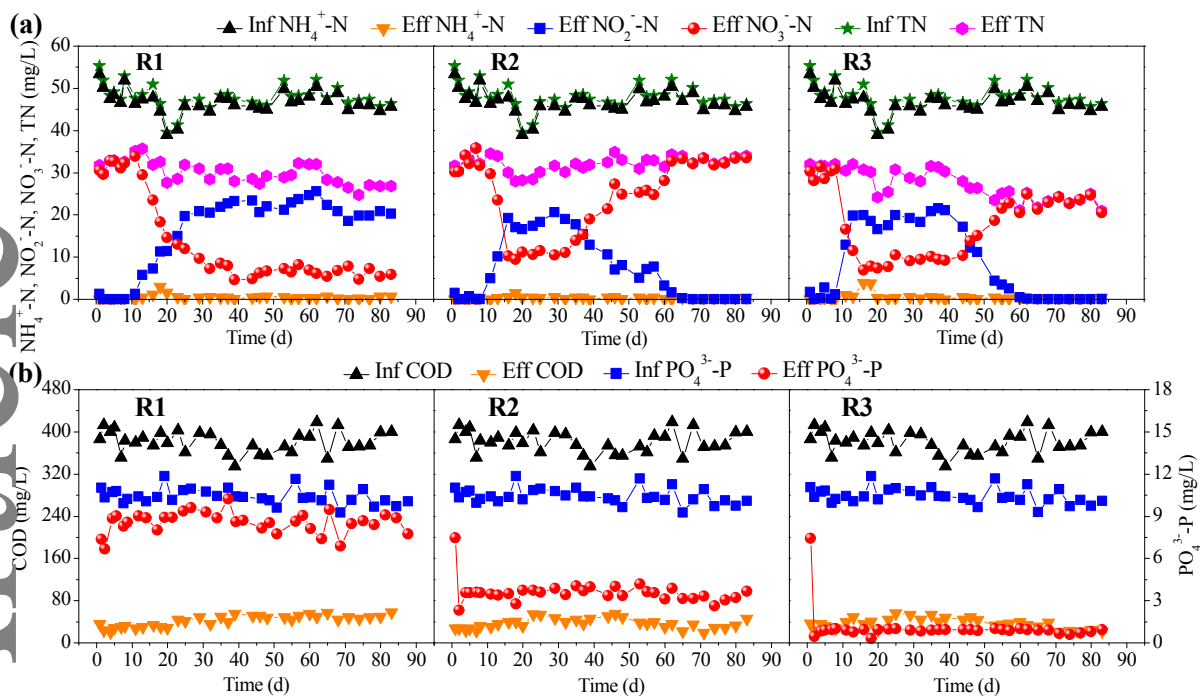


Fig. 4 Variations of NH₄⁺-N, NO₂⁻-N, NO₃⁻-N, TN (a), COD and PO₄³⁻-P (b) concentrations in R1, R2, and R3 during the experimental period

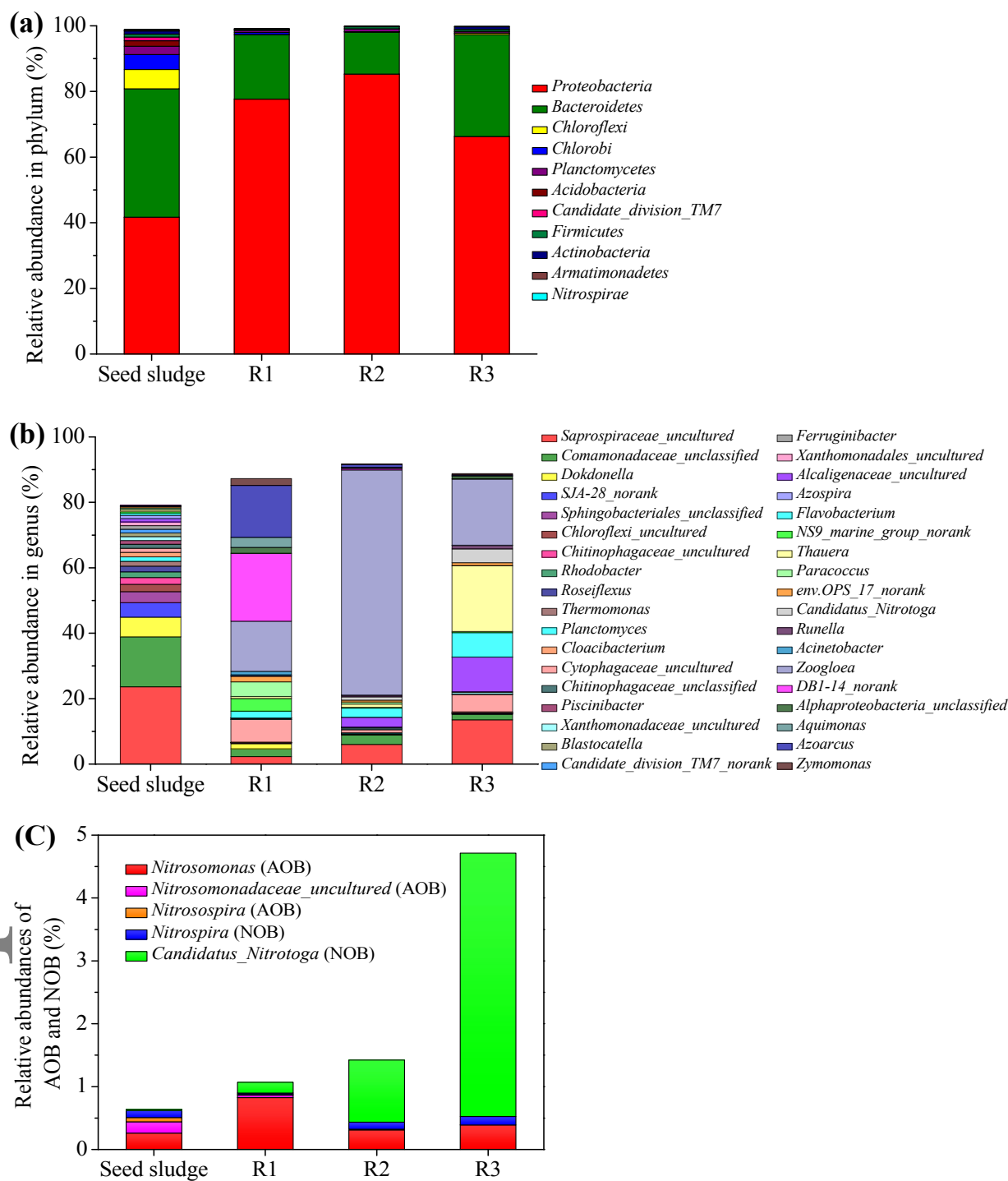


Fig. 5 Microbial community characterization in seed sludge, sludge of R1, R2, and R3 on day 80: (a) relative abundance of community at the phylum level (> 0.1% in at least one sample are listed); (b) relative abundance of community at the genus level (> 1.0% in at least one sample are listed) (c) relative abundance of identified AOB and NOB)